

# Potential Hazard of Aircraft Wake Vortices in Ground Effect with Crosswind

Robert E. Robins\* and Donald P. Delisi†

*Northwest Research Associates, Inc., Bellevue, Washington 98009*

Aircraft wake vortices, evolving close to the ground in a crosswind, are a potential hazard to aircraft landing or taking off on the same or parallel runways. The objective of this work has been to study, by means of numerical simulation, the effect of aerodynamic and environmental conditions on the generation and transport of these vortices. The approach has been to use a computer code which solves the two-dimensional, time-dependent, incompressible Navier-Stokes equations expressed in stream function-vorticity form, to study wake vortices in ground effect with crosswind. The code permits the specification of arbitrary atmospheric stability and wind profiles. A mixed no-slip/free-slip lower boundary condition has been invoked to model the interaction of the vortices with the ground. Comparisons of code output with laboratory and field data have been used to validate the code. Simulation results have shown that, even after evolution times and cross-runway transport distances on the order of 3 min and 500 m, vortices generated by large aircraft close to the ground in a crosswind can carry sufficient average circulation to be a potential hazard to smaller aircraft. Additional full-scale data need to be acquired and additional numerical comparisons need to be performed to assess the significance of these new results.

## I. Introduction

IT is well known that the wake vortices of large aircraft can pose a hazard to closely following smaller aircraft. This hazard is greatest at airports, where aircraft routinely line up to use the same runway, but it is also present at higher altitudes. Less commonly realized is that aircraft taking off or landing on runways that are parallel to runways servicing larger aircraft are also potentially at risk. Wake vortices generated by a large aircraft which is approaching or leaving a runway can survive the interaction with the ground (see below) and be blown by a crosswind into the path of a smaller aircraft operating on a parallel (or the same) runway. This article reports on the results of numerical simulations of how ground interaction and crosswind affect the evolution of an aircraft wake vortex system. Since atmospheric stratification is also known to profoundly affect vortex evolution,<sup>1</sup> measured stratification has been included in the aircraft wake vortex simulations.

Previous studies of vortices in ground effect include the field observations of Pengel and Tetzlaff,<sup>2</sup> Burnham,<sup>3</sup> Dee and Nichols,<sup>4</sup> and Tombach et al.<sup>5</sup> Pengel and Tetzlaff studied the cross-runway transport of wake vortices at the Frankfurt Airport where parallel runways are frequently used. They observed that under stable atmospheric conditions, wake vortices were capable of surviving up to 3.5 min and traveling about 500 m perpendicular to the runway when influenced by crosswinds having mean speeds of 3–5 m/s, measured at a height of 10 m. Among Burnham's findings was the confirmation of Dee and Nichols' earlier findings that wake vortices will separate and rebound upon interacting with the ground. Inviscid theories predict the separation but not the rebound. The study of Tombach et al. focused on vortex breakdown during ground interaction, noting that ground contact frequently led to some form of vortex breakdown, and that the particular form of vortex breakdown known as core bursting usually changes the form of a vortex without destroying it.

Laboratory observations of vortices in ground effect include the studies of Delisi et al.,<sup>6</sup> Ciffone and Pedley,<sup>7</sup> Barker and Crow,<sup>8</sup> and Harvey and Perry.<sup>9</sup> These studies all found, in agreement with the field observations of Burnham, and Dee and Nichols, that wake vortices will separate and rebound when they interact with the ground. Delisi et al. used a tilting water tank to study stratification and vertical shear effects on the ground interaction with two-dimensional vortices and found that either of these effects will reduce the extent of the rebound. (Vertical shear is defined to be the change in the crosswind speed as a function of the vertical coordinate.) They also found that weak vertical shear will cause the downwind vortex to rebound higher than the upwind vortex, and that the reverse will be true in strong vertical shear. This finding is in agreement with the work of Brashears et al.<sup>13</sup> Ciffone and Pedley towed  $\frac{1}{2}$  scale models of B-747 and DC-10 aircraft in water and found that the ground effect caused distortions in the vortex tangential velocity profiles but left the maximum tangential velocities unchanged. Barker and Crow generated two-dimensional vortices in a stationary water tank and observed the rebound effect for a free as well as a solid surface. Conducting their experiments with a half-span rectangular wing in a low-speed wind tunnel, Harvey and Perry used a moving floor to simulate the ground boundary condition.

Theoretical treatments of a vortex pair in ground effect were reported by Peace and Riley,<sup>10</sup> Saffman,<sup>11</sup> Bilanin et al.,<sup>12</sup> and Brashears et al.<sup>13</sup> The first three papers sought an understanding of the phenomenon of vortex rebound. Taken together, their work cast doubt on the finite core size hypothesis suggested by Barker and Crow,<sup>8</sup> and essentially confirmed the qualitative explanation of Harvey and Perry<sup>9</sup> that viscous generation of secondary vorticity was the main ingredient responsible for the rebound. Attempting to explain Barker and Crow's observation of a rebound at both free and solid surfaces, Peace and Riley introduced a viscous displacement mechanism which acts in addition to secondary vorticity at a solid surface and a vorticity diffusion mechanism which acts in addition to the other mechanisms at a solid surface and alone at a free surface. Brashears et al. focus on an explanation for the phenomenon of vortex tilting, which they observed in field studies. Their approach was to study the streamlines arising from the addition of vertical shear to a vortex pair. In agreement with the observations, their results showed that weak vertical shear will cause the downwind

Presented as Paper 89-3400 at the AIAA Atmospheric Flight Mechanics Conference, Boston, MA, Aug. 14–16, 1989; received April 13, 1991; revision received Feb. 7, 1992; accepted for publication Feb. 13, 1992. Copyright © 1991 by the American Institute of Aeronautics and Astronautics, Inc. All rights reserved.

\*Research Scientist, P.O. Box 3027. Member AIAA.

†Senior Research Scientist, P.O. Box 3027. Member AIAA.

vortex to rebound higher than the upwind vortex, and that strong vertical shear will have the opposite effect (cf., Delisi et al.<sup>6</sup>).

None of the theoretical treatments described above follow the development of the rebound phenomenon beyond the point of the initial rebound. (It has come to our attention that in their article, "Interaction of Decaying Trailing Vortices in Spanwise Shear Flow," *Computers and Fluids*, Vol. 15, No. 1, 1987, pp. 77-92, C. H. Liu and L. Ting use a theoretical model based on the concept of "vortical spots" to study the trajectories of trailing vortices in ground effect beyond the point of the initial rebound.) Some field and laboratory observations (e.g., Burnham,<sup>3</sup> Delisi et al.,<sup>6</sup> and Barker and Crow<sup>8</sup>) have shown, however, that after rebounding, vortices may continue to separate while maintaining an approximately constant distance from the surface. Other laboratory observations (e.g., Van Heijst and Flor<sup>14</sup>) have shown that rebounding vortices may relink and even undergo additional rebound. The determining factor appears to be the vortex Reynolds number,  $Re = \Gamma/\nu$ , where  $\Gamma$  is the vortex circulation and  $\nu$  is the kinematic viscosity. The vortices that continue to separate after rebound have higher values of  $Re$  ( $\geq 20,000$ ) than those that relink ( $Re \leq 2,000$ ). The universality of this observation is the subject of further investigation.

Since the main interest in this article is aircraft wake vortices (which have large  $Re$  values), the numerical results presented are for the higher  $Re$  case of vortex rebound followed by continued separation at approximately constant distance from a solid surface. The approach has been to use a computer code which solves the two-dimensional, time-dependent, incompressible Navier-Stokes equations. The code permits the specification of arbitrary atmospheric stability and wind profiles. For vortices out of ground effect, the code has been validated by means of comparisons with laboratory and field data (see Sec. II). To model the interaction of the vortices with the ground, a mixed no-slip/free-slip boundary condition has been used. When applied to realistic conditions, the simulation results confirm the findings of Pengel and Tetzlaff<sup>2</sup> that vortices generated by large aircraft close to the ground in a crosswind can survive after evolution times and cross-runway transport distances on the order of 3 min and 500 m. The results suggest that surviving vortices can possess sufficient strength to be a potential hazard to smaller aircraft operating on the same runway or on parallel runways which are downwind of the larger aircraft. (Note that the numerical results neglect the effects of ambient turbulence, which may have significant effects on vortex decay. Nevertheless, as supported by the results of Pengel and Tetzlaff,<sup>2</sup> there may be times when atmospheric turbulence effects are negligible.)

Section II describes the numerical approach. Sections III and IV contain numerical results for cases with no crosswind and with crosswind, respectively. In Sec. V, simulation results are presented for a realistic parallel runway situation.

## II. Numerical Approach

The computer code used in the study solves the two-dimensional, time-dependent, incompressible Navier-Stokes equations, expressed in stream function-vorticity form. Mean buoyancy and shear effects are included in the equations, and the code permits the specification of arbitrary mean profiles of atmospheric stability and wind. Variations of density in the momentum equations are neglected except where they give rise to buoyancy forces, a simplification known as the Boussinesq approximation. A simple, scale-dependent eddy-viscosity-like damping scheme (greater damping for smaller scales) is used to dissipate energy transferred to small scales of motion.

The model obtains separate solutions for horizontally averaged quantities and for perturbations about these averages. No assumptions are made in the model about the size of the perturbations. The solution method is to represent the horizontal variation of the perturbation quantities in terms of

complex exponential series with coefficients depending on the vertical coordinate  $z$  and time  $t$ . Side boundaries are thus periodic. The top boundary is chosen to be free slip and the bottom boundary is discussed further below. Centered differences are used to approximate vertical derivatives of mean and perturbation quantities, and a leapfrog scheme with periodic averaging of successive time steps is used to advance the solution in time.

The numerical vortices used in the study are specified by means of an initial field of perturbation vorticity. The vorticity distribution for each vortex has Gaussian form, where a separation distance  $2b_0$ , a circulation  $2\pi B_0$ , and a core radius  $r_0$ , specify the distribution. For a complete description of the numerical approach, including equations, see Robins and Delisi.<sup>15</sup>

The treatment of the bottom, or ground, boundary condition is critical to the successful modeling of the interaction between wake vortices and the ground. The conventional method is to use a no-slip condition, but the simulations using this condition were not successful because the coarseness of the computational grid resulted in an overestimate of the viscous interaction at the ground. The boundary condition used for the results presented here was a mixed no-slip/free-slip condition where the vorticity at the ground  $\eta_0$  is specified as

$$\eta_0 = \alpha\eta_N + (1 - \alpha)\eta_F$$

where  $\eta_N$  is the no-slip value of  $\eta_0$ ,  $\eta_F$  is the free-slip value of  $\eta_0$ , and  $0 < \alpha < 1$  where  $\alpha$  may be called the no-slip fraction. As suggested by Roache<sup>16</sup>

$$\eta_N \text{ is chosen to be } -2\psi_1/(\Delta z)^2$$

and  $\eta_F$  is set to  $\eta_1$ , where  $\psi_1$  and  $\eta_1$  are the values of perturbation stream function and vorticity at the first grid point above the ground, and  $\Delta z$  is the vertical grid spacing. The value of  $\alpha$  is chosen by comparing numerical results with laboratory and field data; it was found that  $\alpha$  depends on the vertical grid spacing and the core radius (see below).

The code has been validated in the case of vortex evolution out of ground effect by comparing computed vortex trajectories with laboratory and field measurements, and computed average circulation with field measurements. The average circulation about a vortex  $\Gamma$  up to a radius  $r$  is defined as

$$\Gamma(r) = \frac{1}{r} \int_0^r \Gamma(r') dr'$$

where  $\Gamma(r')$  is the vortex circulation  $2\pi r'V(r')$ ,  $r'$  being the vortex radius and  $V(r')$  the tangential velocity profile.

Robins and Delisi<sup>15</sup> show good agreement between code results and laboratory data for nonstratified and stratified flows, and Delisi et al.<sup>17</sup> show good agreement between code results and laboratory data for a stratified shear flow. The measurements of Burnham et al.<sup>18</sup> were used as the basis for validating the code for the field situation. Figures 1 and 2 show comparisons of code results with vortex trajectory and average circulation data from run 8 of this data set. Measured vortex parameters  $b_0$ ,  $B_0$ ,  $r_0$ , and measured atmospheric stability data measured for this run were used to initialize the code. The comparisons show that the code predicts the trajectory data and the circulation data reasonably well.

## III. Results for Laboratory Vortices in Ground Effect

Delisi et al.<sup>6</sup> and Barker and Crow<sup>8</sup> have shown in laboratory experiments that upon approaching a solid surface in unstratified and unsheared fluid, a vortex pair will separate, rebound, then continue to separate while remaining an approximately constant distance from the surface. Barker and Crow observed this phenomenon at both solid and free sur-

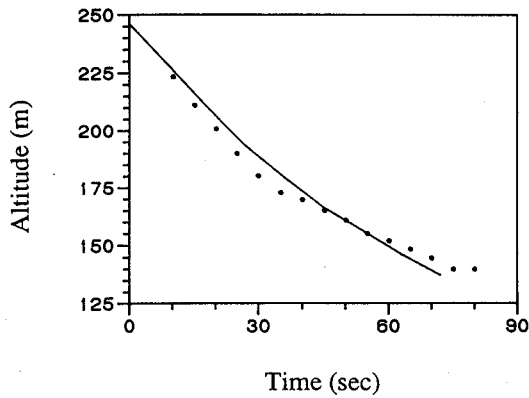


Fig. 1 Comparison of code results (—) with field measurements (•) for run 8 from Burnham et al. (1978).<sup>18</sup>

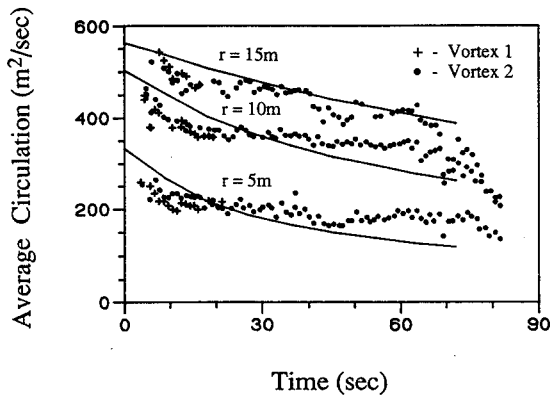


Fig. 2 Comparison of code results (—) with field measurements (+, •) for run 8 from Burnham et al. (1978).<sup>18</sup>

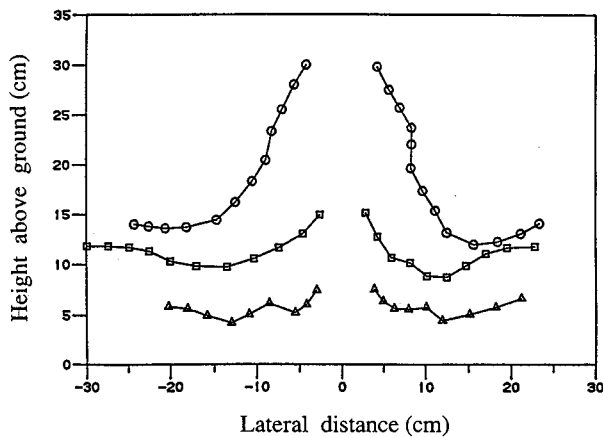


Fig. 3 Laboratory measurements of vortex trajectories from Delisi et al.<sup>6</sup> The circles, squares, and triangles represent measurements for vortices beginning their descent from heights of 34 cm, 17 cm, and 10 cm, respectively.

faces. Figures 3 and 4 show results from Delisi et al. and Barker and Crow, respectively.

Previous theoretical studies by Peace and Riley,<sup>10</sup> Saffman,<sup>11</sup> and Bilanin et al.,<sup>12</sup> discussed in Sec. I, investigated the rebound of a vortex from a solid surface. While all of these studies observed vortex rebound, none followed the vortex rebound to the point (for higher  $Re$  flows) where the vortices continue to separate while maintaining an approximately constant distance from the surface.

In the attempt to simulate the vortex rebound phenomenon, values of  $b_0$ ,  $B_0$ , and  $r_0$  inferred from laboratory observations have been used. At the boundary, a no-slip condition was initially used with the result that there was a very strong rebound without continued motion parallel to the no-slip surface. Flow visualizations such as those shown in Fig. 5 dem-

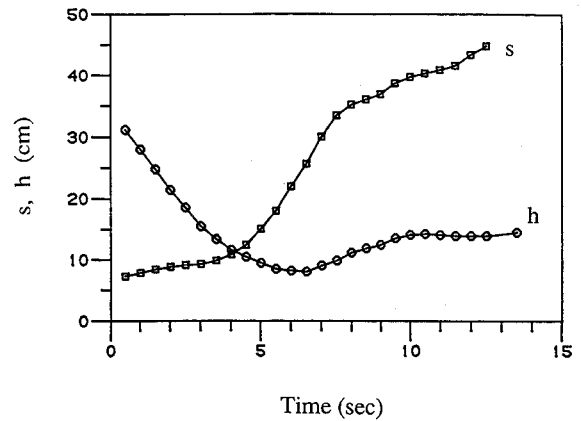


Fig. 4 Laboratory measurements of vortex height ( $h$ ) and half-separation ( $s$ ) vs time, adapted from Barker and Crow.<sup>8</sup>

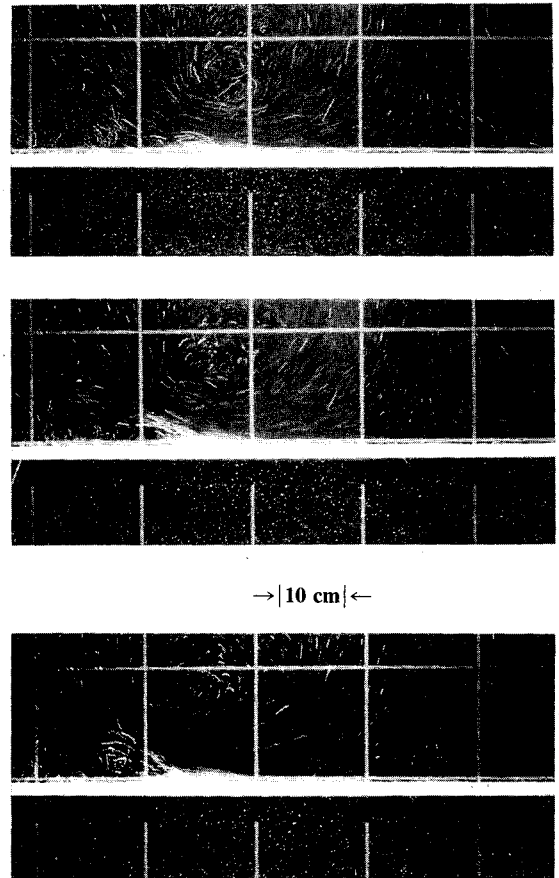


Fig. 5 Sequence of laboratory streak photographs showing the development of a secondary vortex at the floor. The main vortex is clockwise and is migrating toward the floor. Grid lines are 10-cm apart. Flow conditions are nonstratified and nonsheared. Note that as the secondary vortex increases in strength, the main vortex rebounds away from the floor. (From Delisi et al.<sup>6</sup>)

onstrated that the initial viscous interaction was occurring in a layer much thinner than the vertical grid spacing used in the simulation, implying that the no-slip condition was, in fact, exaggerating the viscous interaction.

To simulate the viscous interaction more accurately, the mixed no-slip/free-slip condition described in detail in Sec. II was adopted. In this formulation,  $\alpha$  is the no-slip fraction, and  $(1 - \alpha)$  is the free-slip fraction of the mixed condition. From flow visualizations like those shown in Fig. 5, the thickness of the layer in which viscous effects were dominant was estimated to be about one-eighth of the vertical grid spacing used in the simulation; thus,  $\alpha$  was chosen to be 0.12. The result of using the mixed boundary condition with  $\alpha = 0.12$

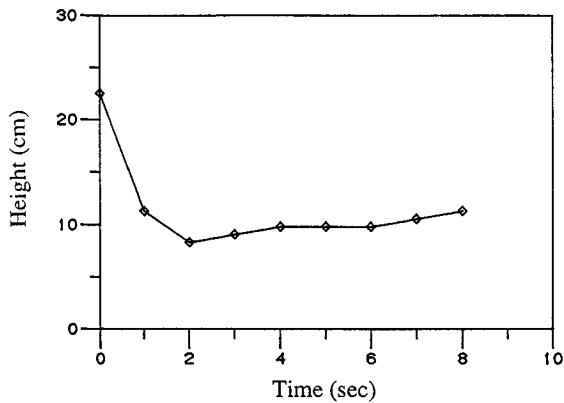


Fig. 6 Computed vortex trajectory resulting from mixed no-slip/free-slip boundary conditions with  $\alpha = 0.12$ .

to simulate the interaction of a vortex pair impinging on a solid surface is shown in Fig. 6. It can be seen that this result displays the same qualitative behavior as the laboratory data, i.e., separation, rebound, and continued separation at approximately constant height.

#### IV. Results for Full-Scale Vortices in Ground Effect with Crosswind

To evaluate the computational approach for a full-scale case, results of numerical simulations were compared with measurements of vortex height, lateral position, and average circulation from a series of B-747 flight tests reported by Burnham.<sup>3</sup> Data from run 1 at Edwards AFB are shown in Fig. 7 and 8. In this case a crosswind holds one of the vortices at a nearly constant lateral position while causing the other vortex to traverse out of the field of view. From the altitude vs time data, the visible vortex is seen to undergo a rebound similar to the rebounds observed in the lab.

In order to simulate these observations, several pieces of information were required. Since the test aircraft was in a landing configuration, a vortex pair is not an adequate description of the vortex wake. Instead, an adaptation of the Betz method was used to model the distribution of vorticity. The Betz method and its extension to complex load distributions is described by Donaldson et al.,<sup>19</sup> and the adaptation is described in the Appendix. An estimate of span loading, which is required by this method, was provided by the Boeing Company. The result was four pairs of vortices (which rapidly roll up into one pair).

Vertical profiles of atmospheric stability and wind are also required by the code. These profiles were obtained from an addendum to Burnham's report. Nominal values, at a height of 20 m, for the stability frequency, the vertical wind shear, and the component of wind velocity across the aircraft flight path, were 25 cyc/h,  $0.007 \text{ s}^{-1}$ , and 25 cm/s.

Remaining code requirements are the form of the scale-dependent damping and a value for  $\alpha$  to establish the boundary condition at the ground. Initially, the damping was chosen to be the same as for the B-747 validation case, described in Sec. 2. This resulted in too much damping at small scales as determined by comparisons with the circulation data, which led to the conclusion that a modified damping model was required for the ground-effect case. Ultimately, the damping for the ground-effect case was chosen to be identical for all scales to the large scale damping used for the out-of-ground-effect case. Evidently, the dynamics of the ground interaction was sufficiently effective in damping small scales so that the additional small-scale damping provided by the code's damping model proved to be excessive.

Since flow visualizations were not available,  $\alpha$  was fixed by the assumption that the effective no-slip fraction,  $\alpha \Delta z / r_0$ , would be invariant. Since the value of this quantity for the lab case was 0.03, and  $\Delta z$  and  $r_0$  for the field case were 1 and 2.5 m,

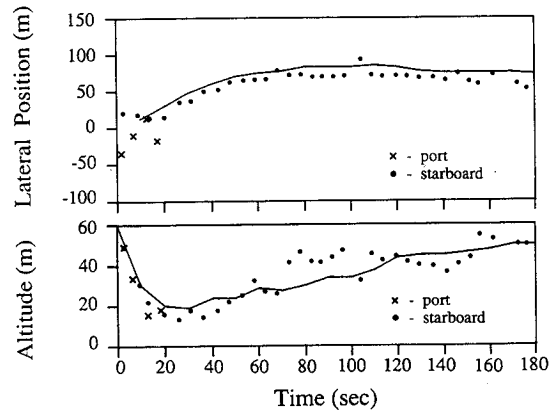


Fig. 7 Comparison of code results (smooth solid lines) with field measurements of vortex motion for run 1 from Burnham.<sup>3</sup>

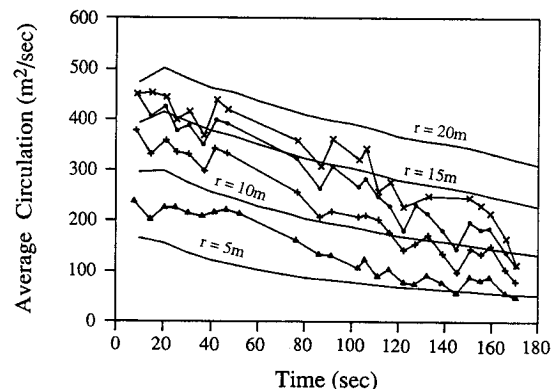


Fig. 8 Comparison of code results (solid lines) with field measurements of average circulation for run 1 from Burnham.<sup>3</sup>

respectively, the value of  $\alpha$  for the field case was 0.075. Results from the code simulation of Burnham's run 1 are superimposed as the solid lines on the field data in Figs. 7 and 8. Good agreement is seen in Fig. 7, and reasonably good agreement is seen in Fig. 8. These comparisons are more impressive when one realizes that the initial wake vorticity distribution was not based on observations of  $b_0$ ,  $B_0$ , and  $r_0$ , as in the previous cases (see Secs. II and III), but on an estimate of the span loading.

Note in Fig. 8 that the field measurements decay rapidly for times greater than 160 s for radii greater than or equal to 10 m. This rapid decay is not modeled well in the calculation. It is not clear, however, whether the rapid decay of the field measurements is due to a physical phenomenon or to measurement error. It is important for airport capacity to determine how long vortices near the ground survive and what their decay mechanisms are. Hence, it is important to determine whether the rapid decay observed in Fig. 8 is physically real. Additional full-scale data need to be obtained to determine the physical mechanisms of vortex decay and to provide a data base for additional numerical simulations.

#### V. Code Simulation of the Vortex Wake of a Landing Aircraft

In this section a description is given of the simulation of the vortex wake of a heavy aircraft on the verge of landing. The motivation for this simulation was an interest in assessing the potential hazard to a smaller aircraft operating on a parallel and downwind runway.

The same damping model and ground boundary condition was used for this simulation as was used for the case in Sec. IV. For the aircraft, a B-767 was chosen, and as in Sec. IV for a B-747, span loading provided by the Boeing Company was used to specify the initial state of the vortex wake. This time the adaptation of the Betz method referred to in the

previous section led to the specification of five vortex pairs from which one pair rapidly formed.

The starting height for the vortices was chosen to be 5 m, a value which corresponds to a time just seconds before touchdown and loss of lift. Vertical profiles of atmospheric stability and wind were chosen from typical atmospheric data recorded at a midwest airport. Nominal values, at a height of 20 m, for the stability frequency, the vertical wind shear, and the component of wind velocity across the aircraft flight path, were 6 cyc/h,  $0.025 \text{ s}^{-1}$ , and 4 m/s. The results from this simulation are shown in Figs. 9–11.

Figure 9 shows the trajectories of the vortices. The effect of the crosswind is clear in the lateral position plot, as both

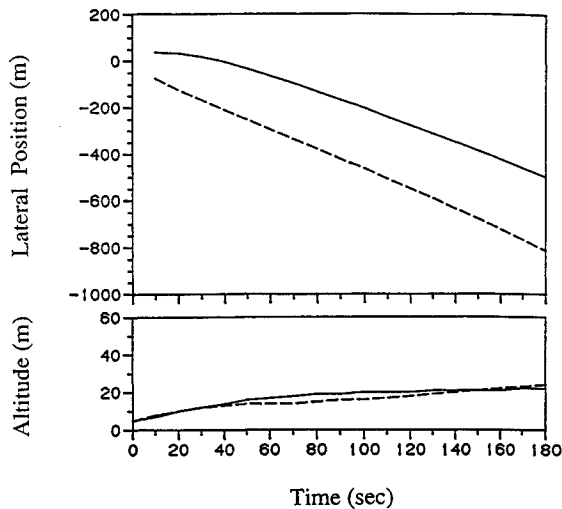


Fig. 9 Numerically calculated trajectories of vortices in the wake of a B-767 aircraft landing in the presence of a crosswind. Lateral and vertical motion of upwind (—) and downwind (---) vortices are shown.

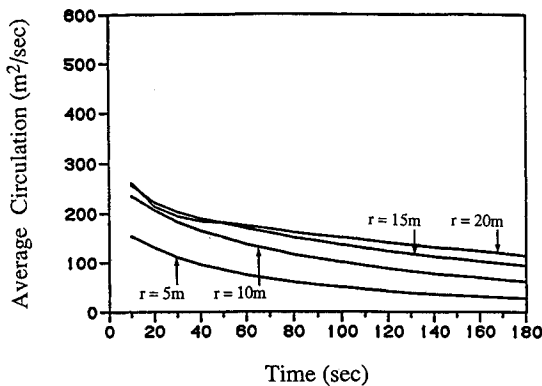


Fig. 10 Numerically calculated average circulation about the upwind vortex whose trajectory is presented in Fig. 9.

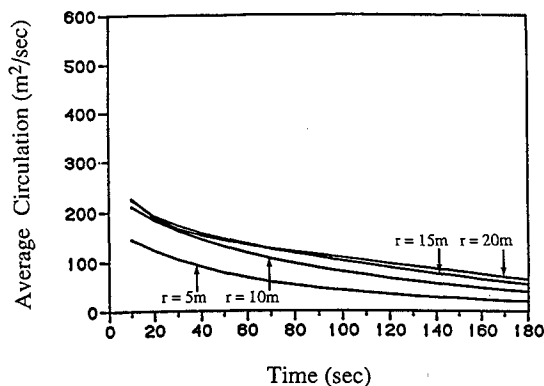


Fig. 11 Numerically calculated average circulation about the downwind vortex whose trajectory is presented in Fig. 9.

vortices are transported in the same direction away from the position of generation. Note that the effect of the crosswind is not simple advection, as the slope of the lateral position vs time relation is less for the upwind vortex than for the downwind vortex. Also note that due to their low generation height, these vortices are immediately in ground effect and so do not “rebound” as did the vortices whose trajectories were shown in Figs. 3, 4, 6, and 7. Average circulation at radii of 5, 10, 15, and 20 m is shown in Figs. 10 and 11 for upwind and downwind vortices, respectively. After 3 min, the upwind vortex has traversed nearly 500 m and its average circulation of radii of 15 and 20 m is in the range  $100\text{--}150 \text{ m}^2/\text{s}$ .

The effect of this amount of average circulation on a following aircraft can be estimated from an analysis presented by Burnham and Hallock.<sup>20</sup> In their report they present an expression for

$$\Gamma_T(b/2)$$

the “vortex strength hazard threshold,” which is the minimum average circulation at a radius of  $b/2$  that a vortex must have to be considered a hazard to a following aircraft of wing span  $b$ . As an example, they show for a DC-9 aircraft ( $b = 30 \text{ m}$ ) that  $150 \text{ m}^2/\text{s}$  is an extreme upper estimate for this threshold (e.g., average circulation values as low as  $75 \text{ m}^2/\text{s}$  might also represent a hazard). It follows from Fig. 10 that the upwind vortex could be considered a potential hazard for a DC-9 aircraft. Similar considerations could be used to show that smaller aircraft are also potentially at risk.

The results therefore imply that the trailing vortices from a B-767 class or larger aircraft which is operating near the ground could potentially pose a hazard for DC-9 or smaller aircraft operating near the ground and downwind from the larger aircraft. If the crosswinds were just strong enough to counteract the cross-runway movement of one vortex and prevent it from traversing away from the runway, then the potential hazard would be to aircraft operating on the same runway.

In summary, the results have shown that aircraft wake vortices in ground effect with crosswind have the potential to be a hazard to other aircraft. Additional field data need to be obtained and analyzed, and corresponding numerical code simulations need to be performed to determine the range of validity of these results and their possible impact on aircraft operations.

#### Appendix: Specification of a Gaussian Vortex Representation for the Rolled-Up Vorticity Downstream of a Wing with Prescribed Loading $\Gamma(y)$

Given the wing loading  $\Gamma(y)$  where  $y$  is the spanwise coordinate, we describe a method for determining the location, strength, and core radius for each of a collection of Gaussian vortices, the intent of which is to approximate the rolled-up vorticity downstream of the wing. Following Donaldson et al.,<sup>19</sup> we first examine the function  $|d\Gamma/dy|$ ,  $0 < y < b$ , where  $d\Gamma/dy$  is conventionally interpreted to be the strength of the vortex sheet downstream of the wing span  $b$ . (We restrict our attention to positive values of  $y$ , since the wing is assumed to be symmetric about  $y = 0$ .) The relative minima of this function partition the domain  $0 < y < b$  into one (if there is only one minimum, located at either 0 or  $b$ ) or more regions. We locate a Gaussian vortex within each of these regions.

Continuing to follow Donaldson et al., we choose the strength of each vortex to be proportional to  $\Delta\Gamma$ —the change in  $\Gamma(y)$  over the region of interest, and we center each vortex at  $\bar{y}$ —the centroid of vorticity within each region. Here  $\bar{y}$  is defined by

$$\bar{y} = \int y \frac{d\Gamma}{dy} \frac{dy}{\Delta\Gamma}$$

where the integral is over the region of interest.

To determine the core radius  $r_0$  for each vortex, we first consider an expression for the vorticity  $\eta$  of a Gaussian vortex whose circulation approaches  $\Gamma$  at large distances from the vortex center. The expression is

$$\eta = (\hat{\Gamma}/\pi r_0^2) \exp(-r^2/r_0^2)$$

where  $r$  is the distance from the vortex center. Making use of the fact that the circulation around a circle is equal to the integral of vorticity over the area enclosed by the circle, it is easily shown that the circulation around the circle of radius  $r_0$  is  $(1 - 1/e)\Gamma$ , which is about  $0.63\Gamma$ .

We use this information to define  $r_0$  for each of the previously considered Gaussian vortices. Our approach is to determine  $\delta$  such that  $|\Gamma(\bar{y} - \delta) - \Gamma(\bar{y} + \delta)|$  is equal to  $(1 - 1/e)\Delta\Gamma$ . We then use this value of  $\delta$  as  $r_0$ . In doing this computation, if  $\bar{y} - \delta$  decreases to the lower bound of the region of interest, we fix  $\bar{y} - \delta$  at this limit and allow  $\bar{y} - \delta$  to continue increasing, and if  $\bar{y} + \delta$  exceeds the upper bound of the region, we fix  $\bar{y} + \delta$  at that limit and allow  $\bar{y} + \delta$  to continue decreasing. In practice, the distance from the centroid to the nearest region boundary is often approximately equal to the rigorously obtained  $r_0$ , and so for simplicity we take  $r_0$  to be this distance.

The wing loading is often given in terms of  $f(y) = c(y)C_L/\bar{c}$  where  $C_L$  is the lift coefficient,  $\bar{c}$  is the average chord length, and  $c(y)$  is the chord length at spanwise coordinate  $y$ . In this case, we can use the fact that  $\Gamma(y)$  is  $0.5V_\infty c(y)C_L$  to express  $\Gamma(y)$  as  $0.5V_\infty \bar{c}f(y)$ , where  $V_\infty$  is the upstream speed. Thus,  $\Delta\Gamma$ , referred to above, is equivalent to  $0.5V_\infty \bar{c}\Delta f$ , and  $\bar{y}$  may be written as  $\bar{y} = \int (df/dy) dy/\Delta f$ .

### Acknowledgments

This study was partially supported by Northwest Research Associates, Inc., Independent Research and Development funds. The authors express their appreciation to the Boeing Company for providing the span loading estimates that were used in the simulations.

### References

- <sup>1</sup>Greene, G. C., "An Approximate Model of Vortex Decay in the Atmosphere," *Journal of Aircraft*, Vol. 23, No. 7, 1986, pp. 566-573.
- <sup>2</sup>Pengel, K., and Tetzlaff, G., "Report of Wake Vortex Measurements with a Ground Wind Vortex Sensing System Using u-v-w Anemometer," Presentation at FAA and NOAA, 1984, Inst. of Meteorology and Climatology, Univ. of Hannover, Hannover, Germany.
- <sup>3</sup>Burnham, D. C., "B-747 Vortex Alleviation Flight Tests: Ground-Based Sensor Measurements," U.S. Dept. of Transportation, FAA Rept. DOT-TSC-FAA-81-19, Washington DC, Feb. 1982.
- <sup>4</sup>Dee, F. S., and Nichols, O. P., "Flight Measurement of Wing Tip Vortex Motion Near the Ground," CP 1065, British Aeronautical Research Council, London, Jan. 1968.
- <sup>5</sup>Tombach, I., Lissaman, P. B. S., Mullen, J. B., and Barker, S. J., "Aircraft Vortex Wake Decay Near the Ground," U.S. Dept. of Transportation, FAA Rept. DOT-TSC-FAA-77-8, Washington, DC, May 1977.
- <sup>6</sup>Delisi, D. P., Robins, R. E., and Fraser, R. B., "The Effects of Stratification and Wind Shear on the Evolution of Aircraft Wake Vortices Near the Ground: Phase I Results," Final Rept. NWRA-87-R006, Northwest Research Associates, Inc., Bellevue, WA, April 1987.
- <sup>7</sup>Ciffone, D. L., and Pedley, B., "Measured Wake-Vortex Characteristics of Aircraft in Ground Effect," *Journal of Aircraft*, Vol. 16, No. 2, 1979, pp. 102-109.
- <sup>8</sup>Barker, S. J., and Crow, S. C., "The Motion of Two-Dimensional Vortex Pairs in a Ground Effect," *Journal of Fluid Mechanics*, Vol. 82, Pt. 4, 1977, pp. 659-671.
- <sup>9</sup>Harvey, J. K., and Perry, F. J., "Flowfield Produced by Trailing Vortices in the Vicinity of the Ground," *AIAA Journal*, Vol. 9, No. 8, 1971, 1659, 1660.
- <sup>10</sup>Peace, A. J., and Riley, N., "A Viscous Vortex Pair in Ground Effect," *Journal of Fluid Mechanics*, Vol. 129, April 1983, pp. 409-426.
- <sup>11</sup>Saffman, P. G., "The Approach of a Vortex Pair to a Plane Surface in Inviscid Fluid," *Journal of Fluid Mechanics*, Vol. 92, Pt. 3, 1979, pp. 497-503.
- <sup>12</sup>Bilanin, A. J., Teske, M. E., and Hirsh, J. E., "Neutral Atmospheric Effects on the Dissipation of Aircraft Vortex Wakes," *AIAA Journal*, Vol. 16, No. 9, 1978, pp. 956-961.
- <sup>13</sup>Brashears, M. R., Logan, N. A., and Hallock, J., "Effect of Wind Shear and Ground Plane on Aircraft Wake Vortices," *Journal of Aircraft*, Vol. 12, No. 10, 1975, pp. 830-833.
- <sup>14</sup>Van Heijst, G. J. F., and Flor, J. B., *Mesoscale/Synoptic Coherent Structures in Geophysical Turbulence*, edited by J. C. J. Nihoul and B. M. Joutar, Elsevier, Amsterdam, 1989, pp. 591-608.
- <sup>15</sup>Robins, R. E., and Delisi, D. P., "Numerical Study of Vertical Shear and Stratification Effects on the Evolution of a Vortex Pair," *AIAA Journal*, Vol. 28, No. 4, 1990, pp. 661-669.
- <sup>16</sup>Roache, P. J., *Computational Fluid Dynamics*, Hermosa Publishers, Albuquerque, NM, 1976, pp. 141 and 145.
- <sup>17</sup>Delisi, D. P., Robins, R. E., and Lucas, R. D., "Initial Laboratory Observations of the Evolution of a Vortex Pair in a Stratified Shear Flow," *Physics of Fluids A*, Vol. 3, No. 11, 1991, pp. 2489-2491.
- <sup>18</sup>Burnham, D. C., Hallock, J. N., Tombach, I. H., Brashears, M. R., and Barber, M. R., "Ground-Based Measurements of the Wake Vortex Characteristics of a B-747 Aircraft in Various Configurations," U.S. Dept. of Transportation, FAA Rept. DOT-TSC-FAA-78-28, Washington, DC, Dec. 1978.
- <sup>19</sup>Donaldson, C. DuP., Snedeker, R. S., and Sullivan, R. D., "Calculation of Aircraft Wake Velocity Profiles and Comparison with Experimental Measurements," *Journal of Aircraft*, Vol. 11, No. 9, 1974, pp. 547-555.
- <sup>20</sup>Burnham, D. C., and Hallock, J. N., "Chicago Monostatic Acoustic Vortex Sensing System, Volume IV: Wake Vortex Decay," U.S. Dept. of Transportation, FAA Rept. DOT-TSC-FAA-79-18, IV, Washington, DC, July 1982.